

Deferoxamine-Induced Bone Dysplasia in the Distal Femur and Patella of Pediatric Patients and Young Adults: MR Imaging Appearance

Yu-leung Chan¹
Chi-kong Li²
Winnie Chiu-wing Chu¹
Lai-man Pang¹
Jack Chun-yiu Cheng³
Ki-Wai Chik²

OBJECTIVE. We investigated the MR imaging appearance of deferoxamine-induced bone dysplasia in the distal femur and patella in patients with thalassemia major.

MATERIALS AND METHODS. Thirty-five patients with homozygous β -thalassemia major who were undergoing regular transfusions and chelation therapy underwent coronal T1-weighted MR imaging of the femur, including the femoral head and the distal femoral epiphysis. Additional coronal fat-saturated dual-echo and sagittal T1-weighted images of the distal femur and patella were obtained in 11 patients who were suspected of having distal femoral lesions on the basis of the coronal T1-weighted images of the entire femur.

RESULTS. No dysplastic change was detected in the proximal femur on coronal T1-weighted images. In 22 distal femurs of 11 patients, the following abnormalities were detected on MR imaging: blurred physal-metaphyseal junction ($n = 22$), distal metaphyseal areas of hyperintensity ($n = 21$), physal widening ($n = 18$), metadiaphyseal lesions ($n = 11$), epiphyseal lesions ($n = 10$), and patellar lesions ($n = 2$). Physal widening and distal metaphyseal hyperintense areas were all more pronounced peripherally. Of the 21 distal metaphyseal hyperintensities, lateral abnormalities were larger than medial abnormalities in 16. Of the 18 distal femurs in which physal widening was detected, the lateral widening was more marked than the medial widening in 12. Patients with MR imaging evidence of bone dysplasia have a significantly ($p = 0.003$) greater height reduction than patients without such evidence of bone dysplasia.

CONCLUSION. Deferoxamine-induced bone dysplasia in the distal femur and patella is represented by a spectrum of morphologic changes in the epiphysis, physis, metaphysis, and metadiaphysis on MR imaging.

Homozygous β -thalassemia major is a heritable disorder of β -globin synthesis that results in the premature death of RBCs. Without treatment, severe anemia and death occur in early childhood. Blood transfusion is the standard treatment for homozygous β -thalassemia major and has improved the quality and life expectancy of these patients during the last 20 years. Regular blood transfusion is commonly complicated by iron overload, which can be reduced by chelation with subcutaneous deferoxamine. Although deferoxamine therapy may induce dysplastic bone changes in the long bones [1–4] that are associated with short stature [1, 3–5], insufficient chelation carries the risk of iron overload that may result in dysfunction of the heart, liver, and endocrine organs. Therefore, chelation therapy must be balanced between the degree of iron overload and the undesirable effect of deferoxamine on bone growth.

The degree of iron overload can be assessed at liver biopsy or noninvasively with MR imaging [6]. Deferoxamine-induced bone dysplasia can be diagnosed when characteristic metaphyseal sclerotic and radiolucent foci are present on conventional radiography [1–4, 7]. Radiographic abnormality lags behind pronounced growth failure by 2–3 years [5]. MR imaging, with its unique ability to image cartilage, is a valuable technique in the evaluation of physal and metaphyseal lesions [8–10]. Nonetheless, we are aware of only one previous case report in the English literature on the MR imaging appearance of deferoxamine-induced bone dysplasia [11]. Our objective was to investigate the MR imaging appearance of deferoxamine-induced bone dysplasia of the femur and patella, and its relationship to growth retardation. The femur was selected for investigation for the following reasons: the distal femoral metaphysis is a frequent site of involvement in deferoxamine-in-

Received November 22, 1999; accepted after revision May 8, 2000.

¹Department of Diagnostic Radiology and Organ Imaging, Prince of Wales Hospital, The Chinese University of Hong Kong, Shatin, N.T., Hong Kong. Address correspondence to Y.-l. Chan.

²Department of Paediatrics, Prince of Wales Hospital, The Chinese University of Hong Kong, Hong Kong.

³Department of Orthopaedics and Traumatology, Prince of Wales Hospital, The Chinese University of Hong Kong, Hong Kong.

AJR 2000;175:1561–1566

0361–803X/00/1756–1561

© American Roentgen Ray Society

duced bone dysplasia [4]; the distal femoral growth contributes to 40% of the overall length of the lower limb [12]; and genu valgum is a well-documented secondary complication [5, 6] that frequently requires surgery for correction [7].

Materials and Methods

MR imaging of the femur was performed in patients with thalassemia who agreed to participate in a study to evaluate the body iron status. The study was approved by the ethics committee of our institution. Informed consent was obtained from the adult patients or the parents of minor children.

The study population comprised 35 patients (19 males, 16 females with an age range of 6–20 years [mean, 12 years]) who had homozygous β -thalassemia major and were receiving regular blood transfusions and chelation therapy with deferoxamine. The deferoxamine dose did not exceed 50 mg/kg of body weight per day (average chelation dose, 32.3 ± 8.04 mg/kg per day). The duration of deferoxamine therapy ranged from 3 years 11 months to 16 years 8 months (mean, 8.1 years). All patients were examined using a 1.5-T MR imager (Gyroscan ACS NT; Philips Medical System, Best, The Netherlands). Coronal spin-echo T1-weighted MR imaging of both femurs, including the femoral heads and the distal femoral epiphyses, was performed using a body coil with the following parameters: field of view, 450 mm; TR/TE, 450/15 msec; section thickness, 10 mm with a 20% gap; and number of excitations, two. In 11 patients with physal or metaphyseal abnormalities suspected on these coronal images, the distal femur and patella were further studied with a knee coil using coronal turbo spin-echo selective fat-saturation (spectral inversion recovery) dual-echo sequences (TR/first-echo TE, second-echo TE, 2000/20, 60; turbo factor, 6), and sagittal spin-echo T1-weighted sequences (TR/TE, 475/15). Both sequences used a 230-mm field of view, a section thickness of 4 mm with a 10% gap, and two excitations.

The analysis of MR imaging findings was based on the 11 patients (5 females, 6 males; age range, 10–17 years; mean, 13.5 years) with evidence of abnormalities of the distal femur. All MR images were interpreted without knowledge of the growth status of the patients.

Results

Of the 35 patients undergoing spin-echo T1-weighted coronal MR imaging of the whole femur, no proximal femoral abnormalities suggestive of bone dysplasia were detected. Physal or metaphyseal abnormalities in the distal femur detected on T1-weighted coronal images consisted of irregular low-signal-intensity foci at the metaphysis or metadiaphysis (Fig. 1A) or physal indistinctness or widening (Fig. 2A).

On the sagittal T1-weighted and coronal fat-suppressed proton density-weighted images,

abnormalities were detected in the distal femoral epiphysis, physis, metaphysis, metadiaphyseal region, and patella. Bilateral abnormalities were seen in the physes (11/11 patients, 100%), metaphyses (10/11 patients, 90.9%), and metadiaphyses (5/6 patients, 83.3%). The distribution of the abnormalities is listed in Table 1. The regional morphologic characteristics are summarized in the following text.

Epiphysis

Abnormalities seen within the epiphyses ($n = 6$, 60%) included irregular foci of hypointensity on T1-weighted images and hyperintensity on fat-saturated proton density-weighted images, located in the central or subchondral zone of the bony epiphysis or at the epiphyseal–physal junction (Fig. 3). Hypointense circumscribed components on both T1-weighted and fat-saturated proton density-weighted images were also noted in the central bony epiphysis in two of these patients. Irregularity in the bony epiphyseal outline facing the physis was detected in five distal femurs (50%) (Fig. 2B).

Physis and Physal–Metaphyseal Junction

Blurring of the physal–metaphyseal junction was detected in all 22 distal femurs (100%) on fat-saturated proton density-weighted images. This was shown as a loss of definition of the hypointense zone of provisional calcification and osteoid formation of the metaphysis by the increase in signal intensity in the juxtaphyseal metaphysis (Fig. 2B), or as a tongue-like extension of the physal hyperintensity into the distal metaphysis (Fig. 1B). In the latter, the physis, intermediate in signal intensity on T1-weighted images and hyperintense on fat-saturated proton density-weighted images, also appeared widened. Physal widening was detected in 18 distal femurs (81.8%). The widening was located at the periphery of the physis in 14 (77.8%) of the 18 femurs (Figs. 2B and 3D) and centrally in four

(22.2%). Of the 14 cases of peripheral physal widening, the lateral widening was more marked than the medial widening in 12 cases (85.7%). The physal widening was confined to the lateral aspect in two (14.3%).

Distal Metaphysis

Distal metaphyseal changes near the physis were hyperintense on fat-saturated proton density-weighted images, and they more frequently involved the peripheral and lateral portions (Fig. 3D). Of the 21 involved distal metaphyses, the lateral hyperintensities were larger than the medial ones in 16 (76.2%). Markedly hyperintense foci consistent with pseudocystic change were detected in 15 distal metaphyses (71.4%) (Fig. 1B).

Metadiaphysis

Abnormalities in the metadiaphyseal region were commonly heterogeneous in signal intensity, consisting of irregular foci that were hypointense on T1-weighted images and hyperintense on fat-saturated proton density-weighted images, and markedly hypointense linear or irregular foci on both T1-weighted and fat-saturated proton density-weighted images ($n = 6$, 54.5%) (Fig. 1). Predominantly linear or irregular hypointense changes were seen in five femurs (45.5%).

Patella

Two patients (18.2%) had abnormal signal changes in their patellae. An intrapatellar circumscribed lesion was detected in one patient (Fig. 3B), and an irregular subchondral outline was seen in the other.

The mean height standard deviation (SD) scores at the time of examination of the 11 patients with MR imaging evidence of deferoxamine-induced changes in the distal femur was -2.96 (2.96 SDs below the 50th percentile value), whereas that of the other 24 patients was

TABLE 1 Distribution of Lesions at Distal Femur

Lesion Type	No. of Femurs Involved ($n = 22$)		
	Total	Bilateral Changes	Unilateral Changes
Epiphyseal lesion	10	8	2
Physal–metaphyseal junction blurring	22	22	
Physal widening	18	18	
Distal metaphyseal lesions	21	20	1
Distal metaphyseal pseudocystic change	15	14	1
Metadiaphyseal lesions	11	10	1
Patella lesions	2		

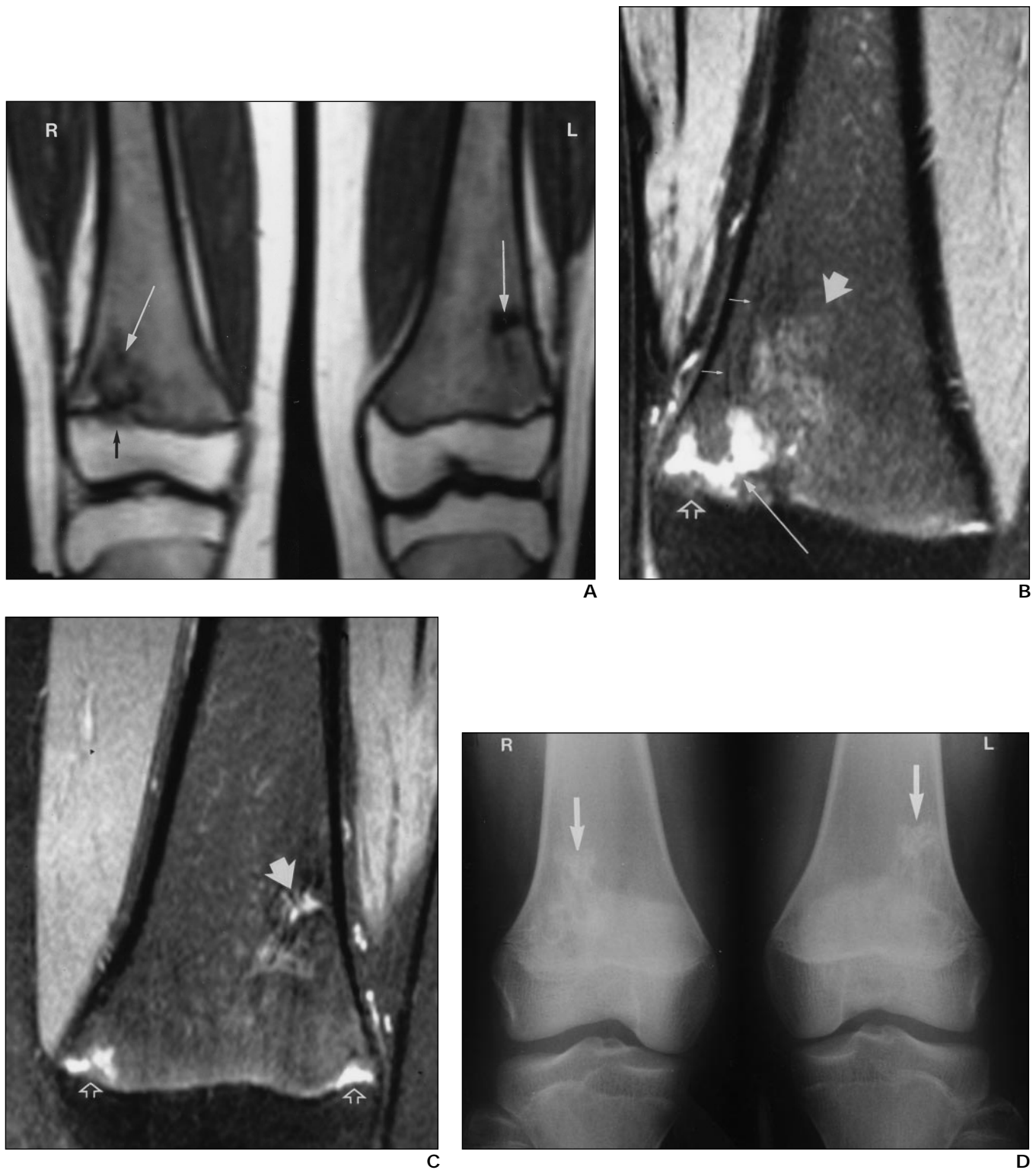


Fig. 1.—16-year-old girl who underwent chelation therapy for 9 years. Her height was at third percentile at time of MR imaging.
A, Coronal spin-echo T1-weighted image (TR/TE, 450/15) of distal femurs shows interruption of hypointense band between epiphysis and metaphysis by intermediate-signal-intensity focus (*black arrow*, R) that extends into and merges with hypointense change at metaphysis (*white arrow*, R) on right side. Hypointense lesion (*white arrow*, L) is seen in metadiaphyseal region on left side.
B, Fat-saturated proton density-weighted MR image (2000/20) of right distal femur shows hyperintense lesion (*open arrow*) extending from physis into metaphysis marked laterally. Pseudocystic transformation is suggested by hyperintense change (*long arrow*). Note mixed hyperintensity (*thick arrow*) and areas of linear hypointensity (*small arrows*).
C, Coronal fat-saturated proton density-weighted MR image (2000/20) of left distal femur shows hyperintense lesions at both medial and lateral margins of physis and distal metaphysis (*open arrows*) that are smaller than lesions seen in **B**. Mixed hyper- and hypointensities are seen at metadiaphyseal region laterally (*solid arrow*).
D, Radiograph shows sclerosis (*arrows*) at both distal femoral metaphyses. R = right, L = left.

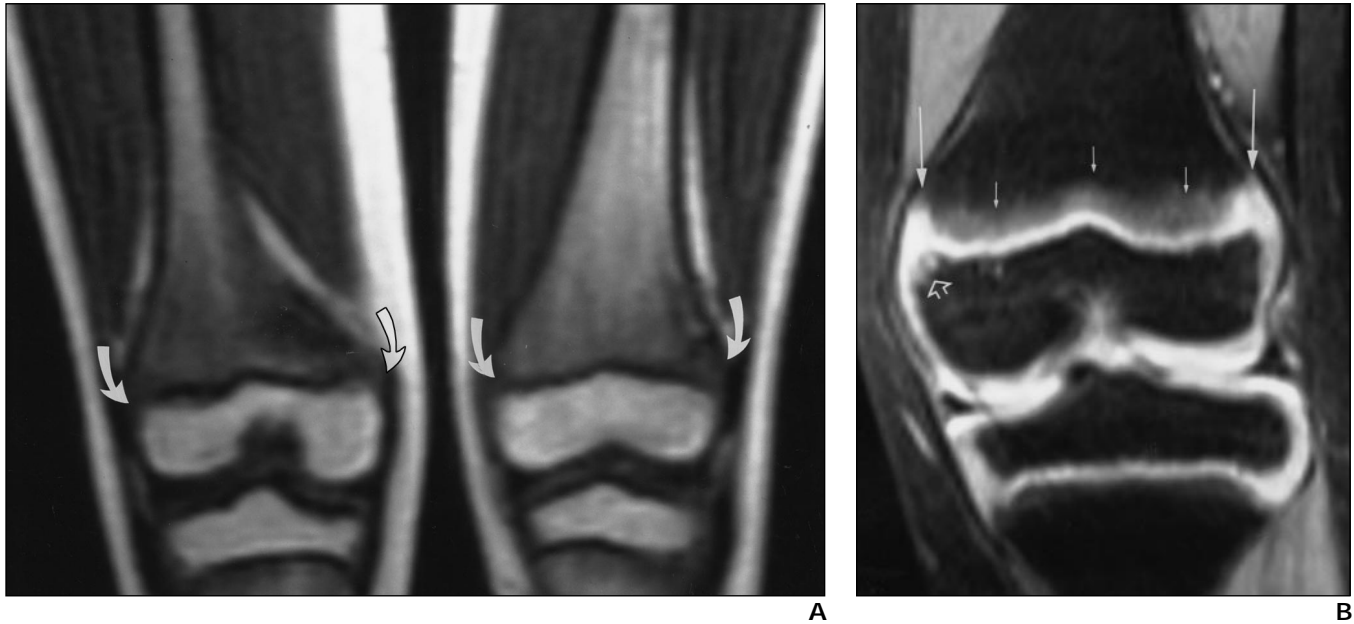


Fig. 2.—10-year-old girl who underwent chelation therapy for 7 years 5 months. Her height was 6 cm below third percentile at time of MR imaging. **A**, Coronal spin-echo T1-weighted image (TR/TE, 450/15) of distal femurs shows widening of intermediate-signal-intensity physis at both medial and lateral margins bilaterally (arrows). **B**, Fat-saturated proton density-weighted MR image (2000/20) of left distal femur shows increase in signal intensity of juxtaphyseal metaphysis, blurring of physal-metaphyseal junction (short arrows), and widening of physis at both medial and lateral margins (long arrows). Slightly irregular outline is observed at medial corner of epiphysis facing physis (open arrow).

–1.33. The difference in height SD scores between the two groups is statistically significant ($p = 0.003$, Mann-Whitney test). Although the mean duration of deferoxamine therapy was slightly longer in the 11 patients with dysplasia (range, 7 years 6 months to 14 years 2 months; mean, 8.9 years) than in the 24 healthy patients (range, 3 years 2 months to 16 years 8 months; mean, 7.7 years), the difference was not statistically significant ($p = 0.09$, Mann-Whitney test). The mean age at the beginning of chelation therapy was 4.6 years (range, 1 year 1 month to 7 years 4 months) and that of the 24 healthy patients was 3.5 years (range, 1 year 11 months to 7 years 6 months). The difference between the two groups was not statistically significant ($p = 0.06$, Mann-Whitney test).

Discussion

In the single case report of the MR imaging appearance of deferoxamine-induced bone dysplasia [11], areas of high-signal change on T2-weighted images and of low signal intensity on T1-weighted images at the metaphyseal region were shown to correspond to areas of irregular sclerosis and radiolucency on conventional radiography. In our study, besides metaphyseal changes, deferoxamine-induced lesions were also de-

tected on MR imaging in the epiphysis, physis, and metadiaphyseal region.

Epiphyseal involvement was detected in 10 (45.5%) of 22 femurs with MR imaging evidence of dysplasia, which is more frequent than noted in a previous radiographic study [1]. This greater frequency is probably because of the high sensitivity of MR imaging in detecting bone and cartilage lesions. The subchondral and chondral locations of these abnormalities and their extent can be clearly delineated on MR imaging. The continuity of the chondral lesions with the physal lesion can also be accurately assessed.

Physal widening, a documented feature on radiography [2, 4, 11], is a frequent finding on MR imaging in deferoxamine-induced bone dysplasia in our study. Physal widening may be seen in metaphyseal chondrodysplasia, spondylometaphyseal dysplasia, and myelodysplasia [13], but none of our patients had clinical evidence of these conditions. Furthermore, the more marked lateral peripheral physal widening in our patients is not typical in these dysplasias. Although irregular foci of physal widening may be seen in several metaphyseal chondrodysplasias, the widening is more frequently uniform across the width of the bone [14]. Traumatic insults may result in central or peripheral focal physal widening [10, 15], but none of our patients had a his-

tory of trauma or vigorous exercise. Chronic physal fractures or stress-related physal widening are also unaccompanied by loss of the distinct hypointense line of provisional calcification [13]. Symmetric physal widening in patients with rickets [16] is unlike that seen in our patients.

The normal physal-metaphyseal junction is hypointense and is well defined on MR imaging because it corresponds to the zone of osteoid formation and provisional calcification [17, 18]. In deferoxamine-induced bone dysplasia in the distal femur, the definition of the physal-metaphyseal junction on MR imaging is blurred. This blurring may be a result of abnormal endochondral ossification from interference of the zone of provisional calcification or osteoid formation [19]. Loss of the hypointense line of provisional calcification on MR imaging is documented in rickets [16], which is also characterized by derangement of endochondral ossification.

Distal metaphyseal lesions are shown as areas of juxtaphyseal hyperintensity or as tongue-like extensions from the hyperintense physis on fat-saturated proton density-weighted images. These lesions predominate at the periphery, particularly laterally. The signal intensity may be slightly lower than, equal to, or higher than that of the hyaline physal cartilage. In more severe cases, marked hyperintensity consistent with pseudocystic change is observed. These changes

MR Imaging of Deferoxamine-Induced Bone Dysplasia

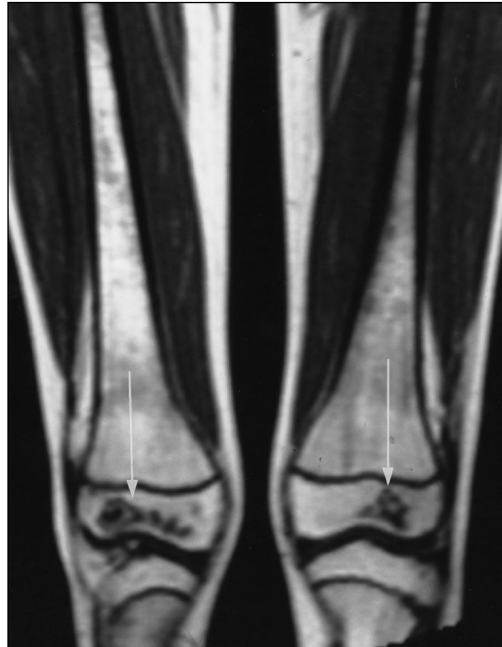
Fig. 3.—13-year-old girl who underwent chelation therapy for 7 years 7 months. Her height was at 10th percentile at time of MR imaging.

A. Coronal spin-echo T1-weighted image (TR/TE, 450/15) of distal femurs shows irregular marked hypointensity (*arrows*) in both epiphyses.

B. Sagittal spin-echo T1-weighted image (450/15) shows hypointense lesions with subchondral extension (*straight arrow*) at distal femoral epiphysis. Bony epiphyseal outline appears irregular. Lamellar area of hypointensity (*curved arrow*) is present in patella.

C. Lateral radiograph shows sclerotic change (*straight arrows*) in epiphysis. Density (*curved arrow*) in corresponding part of patella is only faintly increased. Sclerosis is present at proximal tibial metaphysis.

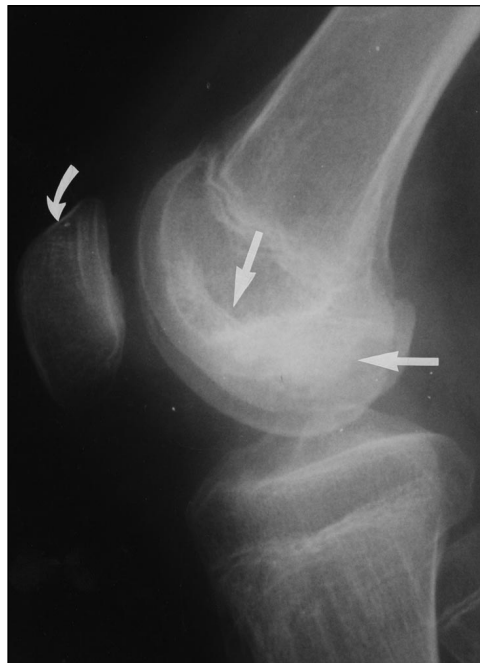
D. Coronal fat-saturated proton density-weighted MR image (2000/20) of right distal femur shows epiphyseal hyperintensity in medial and lateral condyles (*straight arrows*). Also note blurring of physeal-metaphyseal junction and hyperintensity extending into metaphysis at periphery (*curved arrows*). Lateral metaphyseal hyperintensity is larger than medial one. Proximal tibial physeal-metaphyseal region is also affected.



A



B



C



D

are probably caused by defective mineralization or osteoid formation. A tongue-like extension of physeal cartilage into the metaphysis has been described after a Salter-Harris type II epiphyseal injury, in chronic physeal injury in gymnasts [15], and in radiation therapy and chemotherapy-induced physeal changes [10].

The predominantly peripheral involvement of both physeal and metaphyseal lesions in this study is quite characteristic and is consistent

with the radiographic finding of a circumferential deficiency of bone at the periphery of the metaphysis [2]. Although we did not obtain sagittal fat-saturated proton density-weighted images to evaluate directly the anterior and posterior margins of the distal femur, metaphyseal hyperintensity and physeal widening could be detected at the most anterior section of the coronal fat-saturated proton density-weighted images. This finding would suggest

that the disease process might be circumferential. Metaphyseal changes that are hypointense on T1-weighted images and hyperintense on T2-weighted images have also been shown to correspond to the metaphyseal radiolucencies characteristic of deferoxamine-induced dysplastic changes on radiography [11]. The larger lateral physeal and metaphyseal lesions shown in our study, with their anticipated accentuated interference with bone growth on the lateral side, may

help to explain the association of deferoxamine toxicity with genu valgum deformity [3–5].

Metadiaphyseal lesions were heterogeneous in signal with serpiginous or linear hypointensities in our MR imaging study. These lesions correspond to the thin sclerotic lines observed radiographically. The lesions may represent changes that have migrated from the metaphysis to the more proximal locations as growth at the physis continues. Migration of a lesion into the metaphyseal region has been observed in growth plate injury [20], and deferoxamine-induced metaphyseal changes have been observed to extend to the diaphyses on longitudinal follow-up [5].

The linear or irregular low-signal-intensity metaphyseal foci on MR imaging bear some similarity to immature bone infarcts, but the low-signal-intensity margins of infarcts tend to be more serpiginous [21]. In infarction, the high-signal-intensity areas on T2-weighted images are found in the center of the infarct surrounded by the low-signal-intensity margin, whereas the hyperintensities in deferoxamine-induced metaphyseal dysplasia are more scattered and randomly arranged with respect to the hypointense lines. The oblique and random orientation of these hypointense lines is different from the transverse orientation of growth arrest lines.

The mechanism by which deferoxamine affects bone growth is not entirely understood. Chelation of zinc [1, 2] and the antiproliferative effect of deferoxamine may be the underlying pathophysiologic mechanisms [22, 23]. Radiation therapy and chemotherapy have been shown by MR imaging and histology to cause tongue-like extensions of the physal cartilage into the metaphysis [10]. This seems to suggest that the defective endochondral ossification is caused by interference with proliferation. Patients with childhood leukemia who receive cytostatic chemotherapy with or without steroids have been shown to develop circumscribed lesions in the metaphysis and epiphysis on MR imaging [24]. Impaired chondrocyte turnover at the chondroosseous junction is seen in rickets [25], which shares some common imaging features [16] with severe deferoxamine-induced bone dysplasia. Whether chondrocyte turnover is affected by deferoxamine, as it is in rickets, is unknown. It is not likely that deferoxamine affects only chondrocyte proliferation because the subsequently decreased chondrocyte turnover leads to early physal closure [25]. Early physal closure was not a feature in our patients or in those of Brill et al. [2]. The inhibition of proliferation of osteoblasts by deferoxamine [26] may be a factor because osteoid formation and subsequent ossification will be affected.

No dysplastic change was detected in the proximal femur on T1-weighted coronal images of the

entire femur in any of our patients. The lack of dysplastic change may be due to the slower growth rate of the proximal femur compared with that of the distal femur. The distal femoral physis contributes to 70% of the overall length of the femur, whereas the contribution from the proximal femoral physis is 30% [12]. The toxic effect of deferoxamine may be less marked on the proximal femur, which has a lower proliferative activity, or the effect may be mild and undetectable.

Deferoxamine-induced changes in the distal femur on MR imaging are associated with growth retardation. This finding is consistent with findings of a previous study showing that marked radiographic abnormalities of the unossified metaphyseal matrix in deferoxamine-treated thalassemic patients is associated with a decline in height percentile [4]. Therefore, the physal and metaphyseal changes on MR imaging may be considered indicators of interference of height growth from the toxic side effect of deferoxamine.

In conclusion, deferoxamine-induced bone dysplasia in the distal femur and patella is represented by a spectrum of changes on MR imaging, comprising characteristic morphologic lesions in the epiphysis, physis, metaphysis, and metadiaphysis. Familiarity with these features would facilitate the diagnosis of deferoxamine-induced long bone dysplasia. Its sensitivity, noninvasive nature, and absence of ionizing radiation are important factors in choosing MR imaging as the modality of choice for longitudinal monitoring of the side effects of deferoxamine chelation therapy in thalassemic children.

References

- De Virgili S, Congia M, Frau F, et al. Deferoxamine-induced growth retardation in patients with thalassemia major. *J Pediatr* **1988**;113:661–669
- Brill PW, Winchester P, Giardina PJ, Cunningham-Rundles S. Deferoxamine-induced bone dysplasia in patients with thalassemia major. *AJR* **1991**;156:561–565
- Olivieri NF, Koren G, Harris J, et al. Growth failure and bony changes induced by deferoxamine. *Am J Pediatr Hematol Oncol* **1992**;14:48–56
- Orzincolo C, Scutellari PN, Castaldi G. Growth plate injury of the long bones in treated β -thalassemia. *Skeletal Radiol* **1992**;21:39–44
- De Sanctis V, Pinamonti A, Di Palma A, et al. Growth and development in thalassaemia major patients with severe bone lesions due to desferrioxamine. *Eur J Pediatr* **1996**;155:368–372
- Papakonstantinou OG, Maris TG, Kostaridou V, et al. Assessment of liver iron overload by T2-quantitative magnetic resonance imaging: correlation of T2-QMRI measurements with serum ferritin concentration and histologic grading of siderosis. *Magn Reson Imaging* **1995**;13:967–977
- Williams BA, Morris LL, Toogood IR, et al. Limb deformity and metaphyseal abnormalities in thalassaemia major. *Am J Pediatr Hematol Oncol* **1992**;14:197–201
- Laor T, Jaramillo D. Metaphyseal abnormalities in children: pathophysiology and radiologic appearance. *AJR* **1993**;161:1029–1036
- Laor T, Jaramillo D, Hoffer FA, et al. MR imaging in congenital lower limb deformities. *Pediatr Radiol* **1996**;26:381–387
- Laor T, Hartman AL, Jaramillo D. Local physal widening on MR imaging: an incidental finding suggesting prior metaphyseal insult. *Pediatr Radiol* **1997**;27:654–662
- Miller TT, Caldwell G, Kaye JJ, et al. MR imaging of deferoxamine-induced bone dysplasia in an 8-year-old female with thalassaemia major. *Pediatr Radiol* **1993**;23:523–524
- Ogden JA. Radiologic aspects. In: Ogden JA, ed. *Skeletal injury in the child*, 2nd ed. Philadelphia: Saunders, **1990**:65–96
- Rodgers WB, Schwend RM, Jaramillo D, et al. Chronic physal fractures in myelodysplasia: magnetic resonance analysis, histologic description, treatment and outcome. *Pediatr Orthop* **1997**;17:615–621
- Shapiro F. Structural abnormalities of the epiphyses in skeletal dysplasias. In: Buckwalter JA, Ehrlich MG, Sandell LJ, Trippel SB, eds. *Skeletal growth and development: clinical issues and basic science advances*. Rosemont, IL: American Academy of Orthopaedic Surgeons, **1998**:471–489
- Shih C, Chang CY, Penn IW, et al. Chronically stressed wrists in adolescent gymnasts: MR imaging appearance. *Radiology* **1995**;195:855–859
- Ecklund K, Doria AS, Jaramillo D. Rickets on MR images. *Pediatr Radiol* **1999**;29:673–675
- Jaramillo D, Connolly SA, Mulkern RV, et al. Developing epiphysis: MR imaging characteristics and histologic correlation in the newborn lamb. *Radiology* **1998**;207:637–645
- Harcke HT, Synder M, Caro PA, et al. Growth plate of the normal knee: evaluation with MR. *Radiology* **1992**;183:119–123
- Jaramillo D, Shapiro F. Growth cartilage: normal appearance, variants and abnormalities. *Magn Reson Clin North Am* **1998**;6:455–471
- Jaramillo D, Hoffer FA. Cartilaginous epiphysis and growth plate: normal and abnormal MR imaging findings. *AJR* **1992**;158:1105–1110
- Munk PL, Helms CA, Holt RG. Immature bone infarcts: findings on plain radiographs and MR scans. *AJR* **1989**;152:547–549
- Lederman HM, Cohen A, Lee JW, Freedman MH, Gelfand EW. Deferoxamine: a reversible S-phase inhibitor of human lymphocyte proliferation. *Blood* **1984**;64:748–753
- Estrov Z, Tawa A, Wang XH, et al. In vitro and in vivo effects of deferoxamine in neonatal acute leukemia. *Blood* **1987**;69:757–761
- Pieters R, Brenk I, Veerman AJP, et al. Bone marrow magnetic resonance studies in childhood leukemia: evaluation of osteonecrosis. *Cancer* **1987**;60:2994–3000
- Farnum CE, Wilsman NJ. Growth cellular function. In: Buckwalter JA, Ehrlich MG, Sandell LJ, Trippel SB, eds. *Skeletal growth and development: clinical issues and basic science advances*. Rosemont, IL: American Academy of Orthopaedic Surgeons, **1998**:203–223
- Tzanno-Martins C, Naves ML, Elorriaga R, Fraga PM, Jorgetti V, Cannata JB. Evaluating the effect of desferrioxamine on bone cell proliferation. *Nephrol Dial Transplant* **1995**;10:714–715